



## Estimating extreme areal precipitation in Norway from a gridded dataset

Anita Verpe Dyrddal, Thomas Skaugen, Frode Stordal & Eirik J. Førland

To cite this article: Anita Verpe Dyrddal, Thomas Skaugen, Frode Stordal & Eirik J. Førland (2016) Estimating extreme areal precipitation in Norway from a gridded dataset, Hydrological Sciences Journal, 61:3, 483-494, DOI: [10.1080/02626667.2014.947289](https://doi.org/10.1080/02626667.2014.947289)

To link to this article: <https://doi.org/10.1080/02626667.2014.947289>



Published online: 15 Dec 2015.



Submit your article to this journal [↗](#)



Article views: 667



View related articles [↗](#)



View Crossmark data [↗](#)



Citing articles: 6 View citing articles [↗](#)

## Estimating extreme areal precipitation in Norway from a gridded dataset

Anita Verpe Dyrørdal<sup>a,b</sup>, Thomas Skaugen<sup>c</sup>, Frode Stordal<sup>b</sup> and Eirik J. Førland<sup>a</sup>

<sup>a</sup>The Norwegian Meteorological Institute, Oslo, Norway; <sup>b</sup>Department of Geosciences, University of Oslo, Oslo, Norway; <sup>c</sup>Norwegian Water Resources and Energy Directorate, Oslo, Norway

### ABSTRACT

To obtain estimates of extreme areal precipitation in Norway, the Norwegian Meteorological Institute currently applies a statistical method that combines measured point precipitation, empirical growth factors, and areal reduction factors. We here suggest performing statistical analysis directly on areal 24-h precipitation from a gridded dataset covering the period from 1957 to the present. Grid-based methods provide increased objectivity and consistency, and enable estimation in ungauged catchments. The proposed method fits the generalized extreme value (GEV) distribution to areal precipitation series in order to estimate precipitation return levels required for design values for flooding and dam safety. The study includes an investigation of the spatial variation of extreme precipitation in Norway, as reflected by the GEV shape parameter. Our results suggest that this parameter varies spatially according to the dominating precipitation systems and, most probably, to the degree of orographic enhancement.

### ARTICLE HISTORY

Received 4 December 2012  
Accepted 16 May 2014

### EDITOR

D. Koutsoyiannis

### ASSOCIATE EDITOR

C. Onof

### KEYWORDS

extreme precipitation;  
Norway; areal precipitation;  
GEV; precipitation; gridded  
data

## 1 Introduction

Estimates of extreme precipitation are decisive for planning and design of important infrastructure, such as reservoir dams, water control systems, urban runoff and transport lines. The accuracy of extreme precipitation estimates is therefore crucial in both economic and safety contexts. Extreme precipitation in regions with varied topography, like Norway, is caused by convective small-scale systems as well as larger-scale frontal systems, subject to orographic enhancement (Roe 2005). The relatively sparse station network also adds to the complexity. Estimates of extreme precipitation are usually presented as values with low frequency or long return periods. For dam design and flood estimation in Norway, the probable maximum precipitation (PMP) is applied along with the 500- or 1000-year return levels, depending on the danger potential (NVE 2011). The authorities responsible for roads, railways and urban planning are more concerned with short-term and intense precipitation with return periods of 5–200 years. For design purposes there is a constant demand for higher temporal resolution, but the lack of sub-daily precipitation measurements often makes it more appropriate to rely on the scaling of daily precipitation.

For most purposes, there is a need for precipitation integrated over an area, introducing a number of challenges because precipitation is associated with large spatial variability. As stated by Skaugen *et al.* (1996), extreme areal precipitation will be a sum of variables, partially from the parent distribution and partially from the distribution of its extremes. Skaugen *et al.* (1996) also describes how the central limit theorem applies when the point process is spatially independent,

implying that the distribution of areal precipitation converges to a Gaussian as the area increases and spatial correlation is reduced. Simultaneously, the extremes of the same distribution will converge to one of three types of the generalized extreme value (GEV) distribution. In the current study we explore the spatial distribution of extreme precipitation at points and areas in Norway, and present a method for estimating extreme areal precipitation in Norwegian catchments.

According to Hanssen-Bauer *et al.* (2009), an increase in annual precipitation was observed over the entire country throughout the last century, and particularly since the end of the 1970s. Further, the frequency and intensity of extreme precipitation events are projected to increase (Hanssen-Bauer *et al.* 2009, Seneviratne *et al.* 2012). The intensity of rainfall-induced floods is thus expected to increase, and higher temperatures will probably lead to a shift towards earlier spring floods and increased possibility of floods during late autumn and winter (Hisdal *et al.* 2006, Hanssen-Bauer *et al.* 2009, Wilson *et al.* 2010). Due to these observed and projected changes, existing design criteria for infrastructure should be revised. Svensson and Jones (2010) found that there is no obvious preferred method for estimating extreme areal precipitation, but that most countries use some kind of regionalization to transfer information from one location to another.

The Norwegian Meteorological Institute (MET Norway) has a national responsibility for providing estimates of extreme areal precipitation estimates in Norway. The present approach (Førland and Kristoffersen 1989, Førland 1992) is a modified version of a method developed by the UK Natural

Environment Research Council (NERC 1975). The method is based on point measurements at meteorological stations and uses empirical growth factors to derive estimates for longer return periods. The method is referred to herein as the station-based growth factor method (SB-gf). Estimation is time-consuming as it requires several manual steps, including subjective measures that influence the result significantly. The latter also leads to a lack of consistency.

We therefore propose a new method for estimating extreme areal precipitation statistics based on daily precipitation interpolated on a 1 km × 1 km grid (Tveito *et al.* 2005, Jansson *et al.* 2007, Mohr 2009) and the GEV distribution. The proposed method is referred to herein as the grid-based GEV method (GB-GEV). An immediate benefit of GEV over growth factors is the possibility for a direct uncertainty measure in terms of confidence intervals. Fine-scale grids have the advantage of providing spatially continuous datasets and a simplified basis for estimates in ungauged catchments. Additionally, downscaled climate projections exist on a similar grid, which enables estimation of extreme precipitation for future climate conditions. To our knowledge, we are the first to use fine-scale grids directly in the estimation of areal precipitation return levels. In Section 2 we describe the development of the alternative method, including an investigation of the GEV shape parameter in Norway. Section 3 provides results from the method comparison and a discussion, followed by conclusions in Section 4.

## 2 From station-based to grid-based estimates

In this section we briefly describe the existing station-based method for estimating extreme areal precipitation, and then

show the basic principles of the proposed grid-based method. The two methods, SB-gf and GB-GEV, are presented in Fig. 1 and the terminology is further explained in the text.

### 2.1 SB-gf

In the UK Flood Studies Report (NERC 1975) a comprehensive statistical analysis was performed on a large rainfall dataset. Empirical growth factors were developed, describing precipitation with a  $T$ -year return period (MT) as a function of M5 (precipitation with a 5-year return period), also called the index value. The ratio MT/M5, referred to as the growth factor. M5 for a 'representative point' within the area, is estimated by the Gumbel-method (Gumbel 2004), equivalent to fitting a GEV type I distribution, and MT is computed in the following way:

$$MT = M5e^{C(\ln(T-0.5)-1.5)} \quad (1)$$

The factor  $C$  is determined empirically as a function of M5, and varies geographically. Analyses performed by Førlund (1987) suggest that values defined for Scotland and Northern Ireland are suitable for Norwegian conditions. For 24-h precipitation with M5 between 25 and 350 mm,  $C$  may be approximated by:

$$C \sim 0.3584 - 0.0473 \ln(M5) \quad (2)$$

Growth factors are used along with standardized areal reduction factors (ARF) (NERC 1975, Bell 1976), converting point values to areal values, and together they constitute the method we here call SB-gf.

The implementation of growth factors from the UK (NERC 1975) at MET Norway more than 30 years ago was

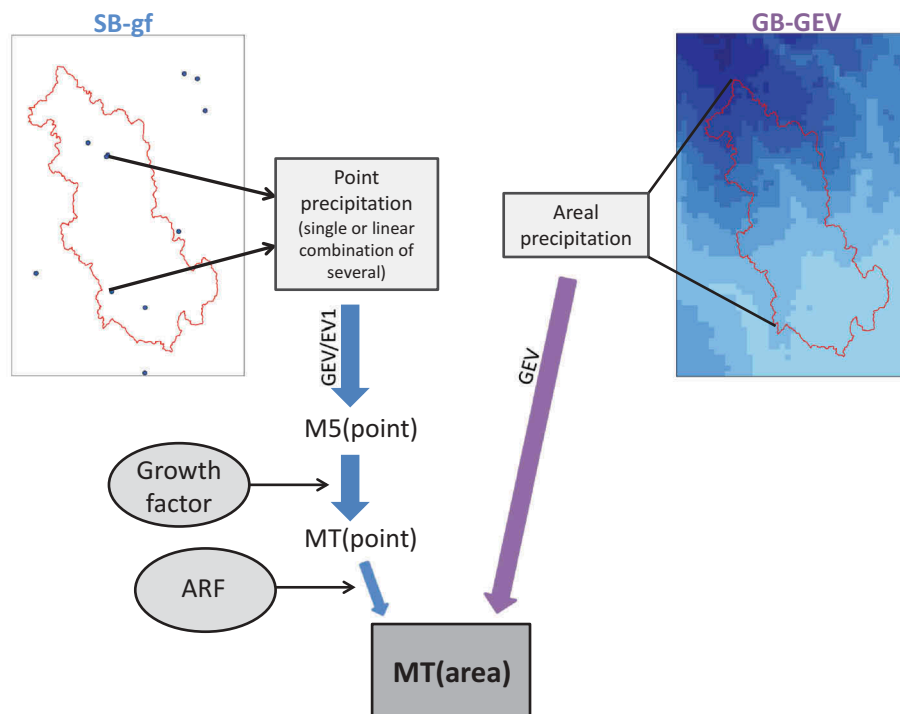


Figure 1. Flowchart of the two methods for estimating extreme areal precipitation: SB-gf and GB-GEV.

motivated by their relatively simple execution at the time, the large amounts of data and the extensive statistical analysis behind them. Because computer power has increased considerably, the use of empirical growth factors may not be the optimal approach today. However, growth factors were originally developed for point precipitation and application to areal precipitation might violate the statistical assumptions on which they are based.

We want to improve the methodology for estimating extreme areal precipitation by moving from point precipitation from meteorological stations (station-based) to areal precipitation from the gridded dataset (grid-based), and from growth factors to the GEV distribution. As areal time series are applied directly, the ARFs then become redundant.

## 2.2 Precipitation grid

Estimates of daily precipitation for the Norwegian mainland are available at MET Norway for the period 1957 until today ([www.seNorge.no](http://www.seNorge.no)). The data are obtained from observations at approximately 400 precipitation stations, interpolated on a 1 km × 1 km grid (Tveito *et al.* 2005, Jansson *et al.* 2007, Mohr 2009). The operational periods of the different precipitation stations vary, as does the collection of measurements used in the interpolation from day to day. Triangulated irregular networks (TINs) are applied in the interpolation: an elevation TIN based on the altitude at the meteorological stations and a precipitation TIN based on measured precipitation. A terrain adjustment is performed, assuming that precipitation increases by 10% per 100 m up to 1000 m a.s.l. and by 5% per 100 m above that. The gridded dataset is used operationally, e.g. in flood forecasting in Norway.

Uncertainties associated with the gridded dataset are mainly related to the interpolation procedure, which in areas with rough topography is particularly challenging. Precipitation enhancement with elevation is based on a simple model known to be highly inaccurate in some cases. For instance, Engeset *et al.* (2004) and Saloranta (2012) found that the vertical precipitation gradient is exaggerated, leading to overestimation at high elevations and underestimation for some low-elevation areas. In regions with a limited number of stations (mountains and northern regions), the influence of single stations is large and may cause biases in the grid-based results.

## 2.3 The GEV distribution

The GEV distribution, introduced by Jenkinson (1955), describes the three possible types of extreme value distributions for block maxima of any variable (Coles 2001). The distribution of the block maxima converges to a GEV distribution  $G(x)$  as the record length approaches infinity. The three-parameter GEV distribution is of the form:

$$G(x) = \exp\left\{-\left[1 + \xi\left(\frac{z - \mu}{\sigma}\right)\right]^{\frac{1}{\xi}}\right\} \quad (3)$$

where  $\mu$  is location,  $\sigma$  is scale, and  $\xi$  is shape. Depending on  $\xi$ , the GEV distribution converges into one of three types

(defined according to the convention used in Coles 2001): Type I/Gumbel/EV1 ( $\xi = 0$ ), Type II/Fréchet/EV2 ( $\xi > 0$ ), and Type III/Weibull/EV3 ( $\xi < 0$ ).

Over the years, the GEV has become an established and widely-used model in extreme value statistics, and a large variety of analysis tools have been developed. Coles and Tawn (1996) claim the GEV distribution to also be valid for areal precipitation.

Large uncertainty is associated with the estimation of the GEV  $\xi$  parameter, representing a challenge when fitting the GEV model. The uncertainty increases for short time series, which is often the case with meteorological variables. The complex topography and climate in Norway also introduce inhomogeneities, and a mixture of precipitation processes in different parts of the country further complicates the estimation of  $\xi$ . Still,  $\xi$  is essential in extrapolating to longer return periods important for design. The challenge associated with the estimation of  $\xi$  motivates a more thorough analysis of the nature and spatial distribution of this parameter in Norway. Here we refer to  $\xi$  for point and areal precipitation as  $\xi_p$  and  $\xi_a$ , respectively.

## 2.4 The GEV parameter $\xi_p$ in Norway

According to several studies, extreme 24-h precipitation at a point follows a Type II distribution (heavy upper tail;  $\xi_p > 0$ ) (Wilks 1993, Koutsoyiannis and Baloutsos 2000, Katz *et al.* 2002, Coles and Pericchi 2003, Coles *et al.* 2003, Koutsoyiannis 2004a). This distribution also represents the lowest risk for engineering structures, as design values are higher than for Type I and Type III. Wilson and Toumi (2005) give evidence for a universal  $\xi_p$  and are supported by Veneziano *et al.* (2009), who suggest a near-universal  $\xi_p$  only depending on duration. Koutsoyiannis (2004b) studied  $\xi_p$  using several methods of estimation and indicated a value of  $\xi_p = 0.15$  as appropriate for mid-latitude areas of the Northern Hemisphere. Wilson and Toumi (2005) found a mean  $\xi_p$  estimate of 0.10 when fitting a GEV distribution to long daily precipitation records from the UK. Veneziano *et al.* (2009) suggest that a constraint on  $\xi_p$  using theoretical arguments is necessary.

To study the spatial distribution of  $\xi_p$  in Norway, we use the method of maximum likelihood estimation (MLE) (Prescott and Walden 1980). Figure 2(a) presents estimates of  $\xi_p$  in single 1 km × 1 km grid cells for the period 1957–2012. We performed the same analysis using the method of weighted least squares (WLS) (Koutsoyiannis 2004b), with weights equal to the empirical quantiles. This method grants higher importance to the largest values, and was shown by Koutsoyiannis (2004b) to be a better fit to empirical values. The spatial distribution of WLS estimates is similar to that of MLE estimates, thus not shown here. Negative  $\xi_p$  are seen mostly in coastal areas, while continental areas are dominated by positive values, showing the same spatial pattern as seen in the actual observations. In Fig. 3 the empirical distribution from the gridded dataset and observations at 569 sites (cf. Fig. 6) are shown, revealing a near Gaussian distribution of  $\xi_p$  with a mean of 0.02003. The

Gaussian distribution of  $\xi_p$  is in accordance with previous findings, e.g. Papalexiou and Koutsoyiannis (2013).

We further assess the regional variability of  $\xi_p$ , by selecting 18 series with more than 100 years of measurements (cf. Fig. 6) and apply Pearson's Chi-square test (Pearson 1900) with  $\alpha$ -level of 0.05 to test spatial homogeneity between  $\xi_p$  at paired sites. The  $\xi_p$  for six sites in the continental Southeast and six sites in the Southwest shows no significant variation within the separate regions. When we combine these 12 sites and an additional six sites from other parts of the country, significant inhomogeneity is evident, suggesting that a constant and strictly positive  $\xi_p$  is not appropriate for Norway.

It is essential to realize that the GEV and other mathematical distributions are simply models that are supposed to mimic the main features of nature. The complexity of nature and its measurements, however, introduces a number of reasons why our observational series and associated estimates do not strictly follow the theoretical framework of for example, the GEV model. In addition to sampling effects related to short time series and uncertainty associated with non-accurate estimation methods, some of the deviance between observations and theory might be explained by the different processes producing extreme precipitation in Norway. Comparing Fig. 2(a) and (c) reveals that negative  $\xi_p$  estimates are mostly found in areas characterized by higher annual precipitation. In these areas the largest daily precipitation values are mainly produced by stratiform systems in the prevailing westerlies, and the precipitation intensity is enhanced by orographic effects across the Norwegian mountain range. A possible explanation for negative values of  $\xi_p$  may be the rather uniform exposure of precipitation types, and that orographic enhancement modifies the extreme value distribution. Some clues on the latter can be obtained from the literature. Blumen (1990) and Yu and Cheng (2013) found that the extent and degree of orographic enhancement depends closely on local topographic geometry, and Yu and

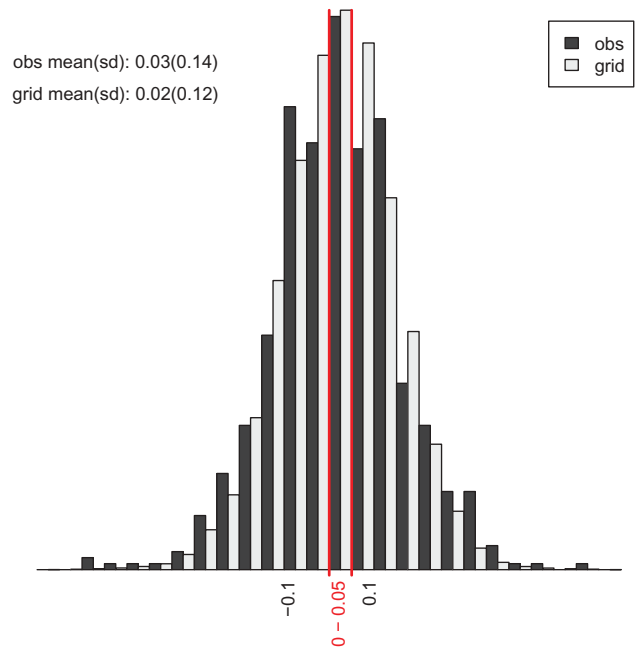


**Figure 3.** Frequency distribution of  $\xi_p$  estimated from observations (dark grey) and the gridded dataset (light grey). The highlighted (red) interval indicates the mean.

Cheng (2008, 2013) found that there are complicated micro-physical interactions between the orographic contribution and the background precipitation from the low pressure system. In addition, Yu and Cheng (2013) suggest that the magnitude of orographic enhancement is not proportional to the background precipitation alone, but to the product of the background precipitation and the wind speed of the oncoming flow. According to Caroletti and Barstad (2010) precipitation in western Norway is dominated by forced uplift, and they show that for stations at some distance from the coast the background precipitation is much smaller than

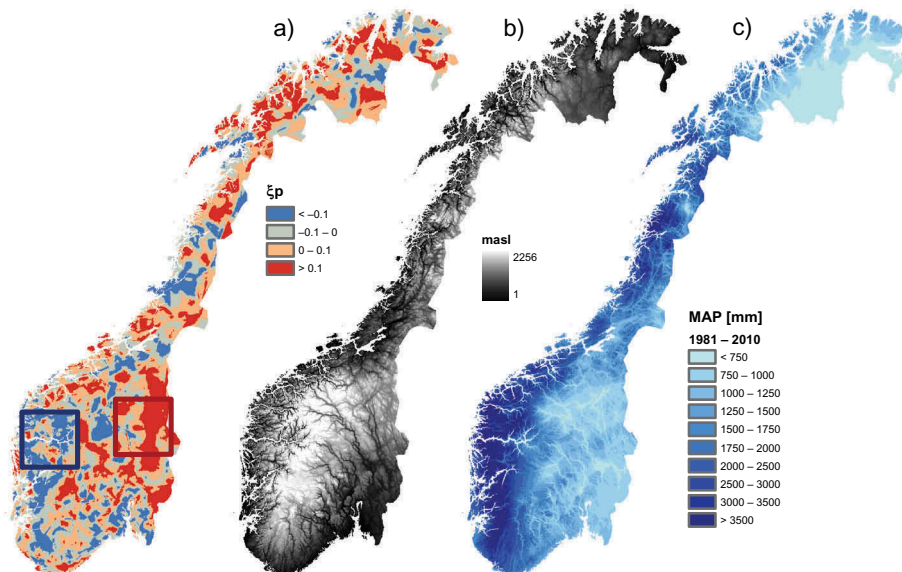


**Figure 2.** (a) Values of  $\xi_p$  estimated from the gridded dataset. The two squares represent areas with mainly positive (red) and negative (blue)  $\xi_p$  and are used in the further analysis. (b) Topography in Norway. (c) Mean annual precipitation for the period 1981–2010.



orographic precipitation during extreme events. It follows that orographic effects influence the distribution of extreme precipitation in these areas. Furthermore, since the mountain range responsible for the forced uplift is static, it is not unreasonable to assume a limit for the orographic effects and hence an upper bound (negative  $\xi_p$ ) for extreme precipitation. In most areas with positive  $\xi_p$ , however, orographic effects are minimal and high-intensity precipitation may occur during frontal systems from the southeast-east sector, and during heavy convective summer showers. These regions thus experience a wider range of precipitation amounts as they are more exposed to mixed-type precipitation systems: isolated convective showers, stratiform frontal systems and embedded convective cells within frontal systems.

In Fig. 4 we further analyse the relationship between  $\xi_p$  and the normal (averaged over the period 1961–1990) annual precipitation (PN), which can be seen as a proxy for the type of dominating precipitation processes. The above statement that  $\xi_p$  decreases with increasing PN is confirmed, and a linear regression shows that this relationship becomes stronger for longer record lengths. For record lengths exceeding 80 and 100 years the fitted slopes are statistically significant at the 0.001 level.

Papalexioiu and Koutsoyiannis (2013) also found that  $\xi_p$  estimates depend on the record length, and show a tendency to higher  $\xi_p$  for longer series. To investigate a possible dependence in Norway we estimated  $\xi_p$  at the 569 observation sites, using both MLE and WLS, and plotted the result against record length (Fig. 5). We divided the 569 series into different lengths to increase the number of series, and computed the median, 5th and 95th quantiles for all lengths for which at least five series were available. We found a weak non-significant positive trend in  $\xi_p$  with record length. The variability is strongly reduced and  $\xi_p$  estimates seem to converge

towards a slightly positive value. WLS estimates are somewhat higher than MLE estimates for all record lengths and have a wider range of values as mentioned above; 62% of WLS estimates are positive, while only 57% of MLE estimates are positive. However, the difference between estimates at single sites seems random, and since WLE does not change the general picture we choose to stay with MLE as our estimation method throughout this study.

## 2.5 The GEV parameter $\xi_a$ in Norway

As mentioned earlier, areal precipitation has a different frequency distribution to point precipitation, and also with regards to extremes. The distribution of extreme areal precipitation is not well studied, mostly because areal precipitation is not a directly measurable variable. As a result of the reduced spatial correlation with increasing area, the parent distribution converges towards a Gaussian due to the central limit theorem. Simultaneously, we expect the extremes of the same distribution to converge towards a GEV Type I ( $\xi_a = 0$ ), which is the domain of attraction of a Gaussian upper tail. This is in accordance with Leadbetter *et al.* (1980), who state that “if  $X_n$  is an independent and identically distributed (i.i.d.) (standard) normal sequence of random variables, then the asymptotic distribution of  $M_n = \max(X_1, \dots, X_n)$  is of Type I”.

Overeem *et al.* (2010) studied  $\xi_a$  from weather radar in the Netherlands. Goodness-of-fit tests were used to show that the GEV distribution fits adequately to areal precipitation data, although the convergence is slower and the need for longer data series is even more crucial. Overeem *et al.* (2010) found that  $\xi_a$  decreases with increasing area, moving from a GEV Type II towards a GEV Type I, and suggest that this may be attributed to the nature of spatial dependence of

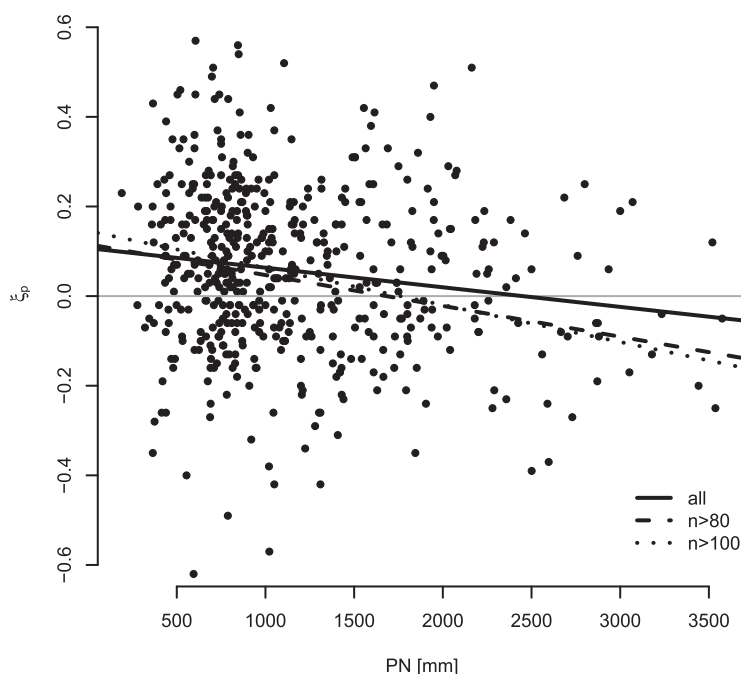


**Figure 4.** Plot of  $\xi_p$  estimated from observations against normal annual precipitation. Linear regression lines for: all series (solid), and series of length >80 years (dashed), and >100 years (stippled). The horizontal (grey) line indicates  $\xi_p = 0$ .

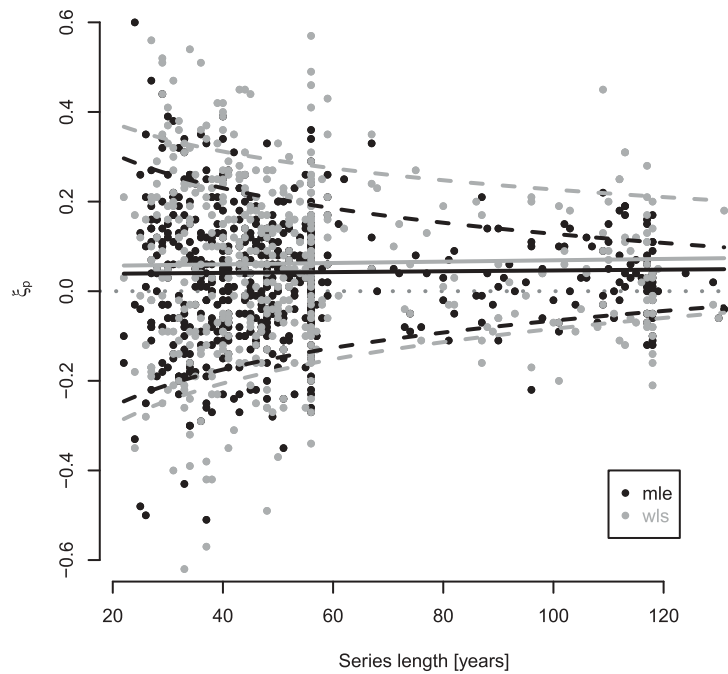


Figure 5. Plot of  $\xi_p$  estimated from observations against time series length.

precipitation. In this section we investigate the behaviour of  $\xi_a$  in Norway using the gridded dataset.

We argued in the previous section that the range of extremes, and thus the  $\xi_p$  parameter, vary according to the dominating precipitation systems and orographic effects. Another aspect for areal precipitation is that different processes and the degree of spatial correlation will create a different population of extremes depending on the size of the catchment. For further analysis we selected 17 catchments in Norway, varying in size from 105 to 5693 km<sup>2</sup>. The catchments were selected according to availability of SB-gf estimates and to represent different parts of the country. They are presented in Table 1 and in Fig. 6.

If the extremes converge towards a GEV Type I in larger areas,  $\xi_a$  would be smaller than  $\xi_p$  in areas where  $\xi_p$  is positive,

and *vice versa*. However, this is not seen in Fig. 7, where we plot the mean  $\xi_p$  against  $\xi_a$  in the catchments. But we note a small tendency to larger differences (deviation from the diagonal) in larger catchments.

To minimize the effects of inhomogeneity, we selected two areas, Southeast and Southwest (see Fig. 2), that are relatively homogeneous in terms of  $\xi_p$ ; positive  $\xi_p$  values dominate the Southeast, while negative values dominate the Southwest. Within these areas we selected 25 points and estimated  $\xi_a$  for increasingly larger areas around the points. Figure 8 reveals a scale-break around 1500 km<sup>2</sup> in both areas, and a second scale-break around 6000 km<sup>2</sup> in the Southeast. These can probably be attributed to the geographical extent of the different precipitation systems that produce extremes in the two areas, and confirm that we are dealing with a mixture of

Table 1. Catchments sorted according to increasing size. Median elevation is taken from the digital elevation model with 1-km resolution applied in the gridded dataset. PN is normal annual precipitation. For size and PN we show values used in SB-gf first, followed by values used in GB-GEV. The percentage difference between PN used in SB-gf and PN used in GB-GEV is given in parentheses.

Catchment	Size (km <sup>2</sup> )	Elevation (m a.s.l.)	PN (mm)	Reference
1. Teksdal	105/107	177	1300/1555 (+19.6%)	Førland (1997)
2. Lauvsnes	114/107	209	1350/1380 (+2.2%)	Isaksen (2006)
3. Aursunda	118/119	260	1300/1398 (+7.5%)	Mamen (2009)
4. Svartevatn	210/204	1046	2050/2748 (+34.0%)	Førland (1991b)
5. Roskreppfjord	282/266	1050	1450/1887 (+30.1%)	Førland (1991b)
6. Vekteren	308/293	610	1250/1118 (−10.6%)	Førland (1991a)
7. Siljan	490/492	220	1050/1157 (+10.2%)	Førland (1986b)
8. Aursjøen	487/496	1280	760/829 (+9.1%)	Hanssen-Bauer (1992)
9. Jølstra	570/573	680	2200/3130 (+42.3%)	Førland (1986a)
10. Namsvatn	696/701	750	1300/1151 (+11.5%)	Førland (1991a)
11. Soneren	701/754	540	900/989 (+9.9%)	Hanssen-Bauer (1991)
12. Sira	1720/1554	693	2020/2529 (+25.2%)	Førland (1991b)
13. Røssvatn	1500/1941	580	1200/1536 (+28.0%)	Førland (1988)
14. Røssåga	1800/1941	580	2000/1536 (−23.2%)	Mamen (2011b)
15. Barduelva	2366/2107	671	575/892 (+55.1%)	Førland (1990)
16. Arendal	4200/4006	520	1150/1290 (+12.2%)	Mamen (2011a)
17. Virdnejavre	5693/5805	435	450/434 (−3.6%)	Førland (1994)

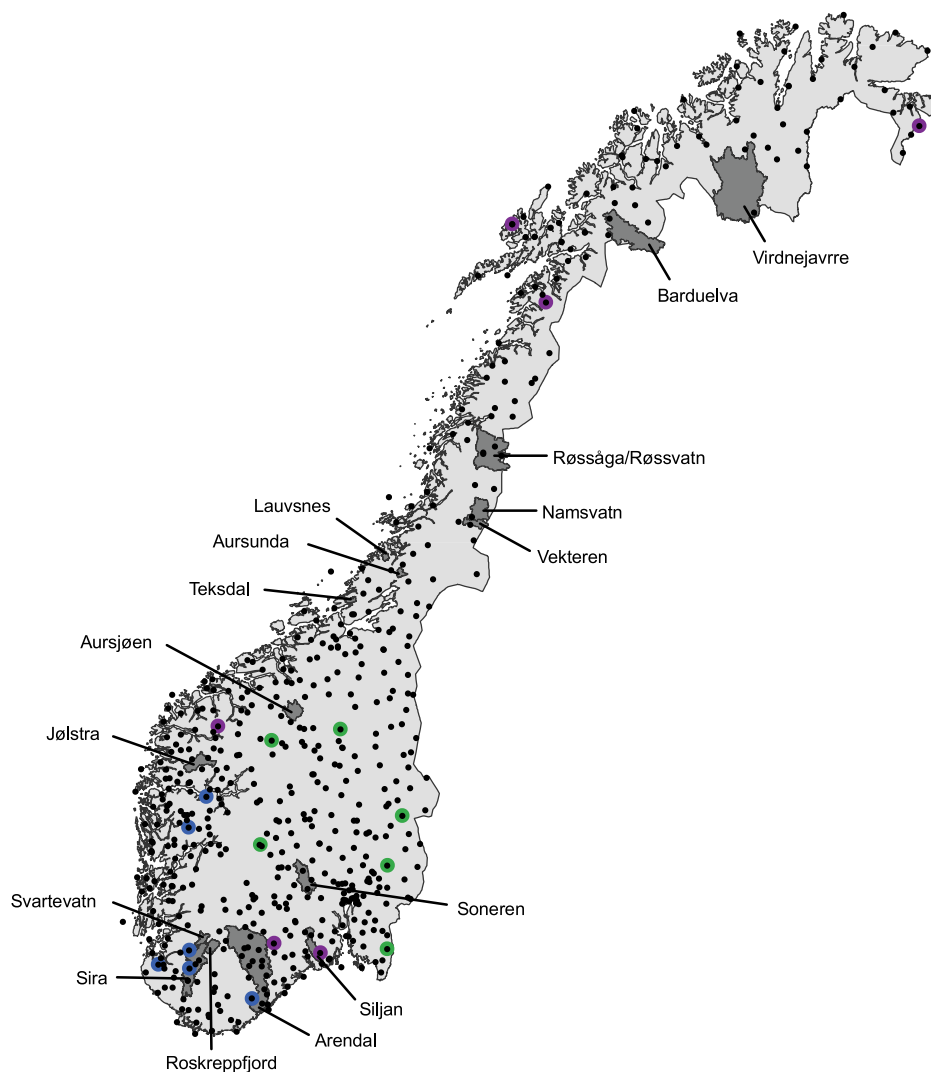


Figure 6. Catchments and observation sites. Coloured sites indicate long (>100 years) observational series separated into regions.

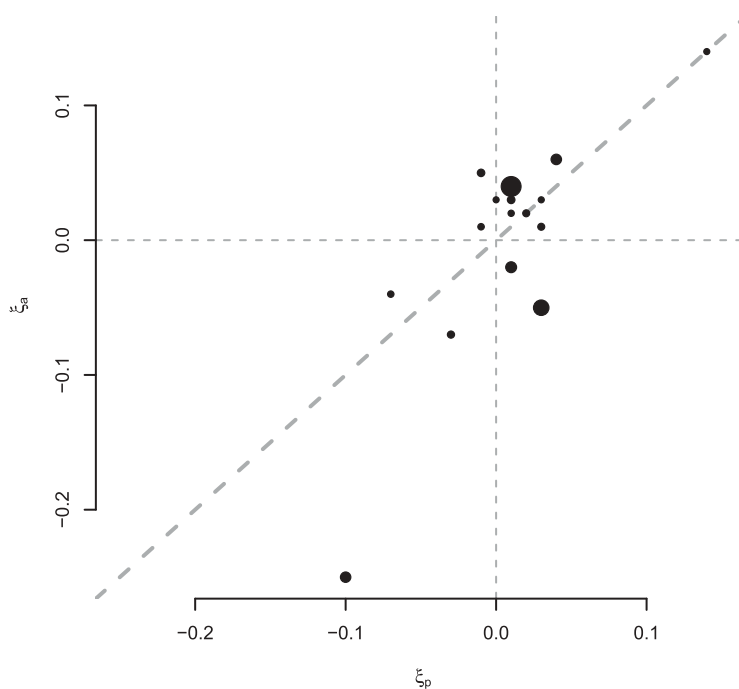


Figure 7. Mean  $\xi_p$  against  $\xi_a$  in the catchments. The size of the dots indicates catchment size. The thick grey dashed line indicates the diagonal ( $\xi_a = \xi_p$ ) and the thin grey dashed lines indicate  $\xi_p = 0$  and  $\xi_a = 0$ .



different extreme value distributions that complicate our study. The two scale-breaks in the Southeast indicate that a greater variety of precipitation types occur here, as suggested in Section 2.4, and that these precipitation types produce extremes from different distributions. After the last scale-break we note that  $\xi_a$  decreases, reflecting the reduced spatial correlation as the area increases. In accordance with Overeem *et al.* (2010), extremes converge from a GEV type II towards a GEV Type I distribution in the Southeast. In the Southwest, however, the Type III distribution is further strengthened. The latter may indicate that in areas of negative  $\xi_p$  the assumptions for the central limit theorem, such as the observations being i.i.d., are not met. A reason for this might be that orographic enhancements have a non-linear and spatially intermittent effect, and hence contaminate the extreme value distribution. These findings have to be considered preliminary and, due to the strong gradients in the Norwegian precipitation climate along with possible misrepresentation of spatial correlation in the gridded dataset, a more thorough investigation of  $\xi_a$  is necessary.

## 2.6 GB-GEV

Our analyses indicate a connection between relevant precipitation indices and the spatial distribution of the GEV  $\xi$  parameter in Norway. We recognize, however, that further work is needed to present a model for  $\xi_a$  according to empirical evidence. As a result, we here choose to estimate  $\xi_a$  directly. The proposed method, GB-GEV, thus includes fitting the GEV distribution to annual maximum areal 24-h precipitation extracted from the precipitation grid, using MLE to estimate the three GEV parameters.

It is common practice to use estimates of probable maximum precipitation (PMP), which represent a precipitation amount with a return period of infinity, in the design of critical constructions such as reservoir dams. Great

uncertainties are associated with the estimation of long return periods, and the development of numerical weather (NWP) models introduces the possibility of perhaps more physically-based PMP estimates (Cotton *et al.* 2003, WMO 2009). Given these considerations we have not attempted a new statistical method for PMP-estimation, but we suggest that a thorough analysis of NWP-based estimation methods is carried out in the future.

## 3 Method comparison and discussion

We compare return level estimates from GB-GEV and SB-gf in the 17 catchments, making use of previously determined SB-gf estimates computed at MET Norway on different occasions (cf. Table 1). Percentage differences for M100, M500 and M1000 are shown in Fig. 9. The GB-GEV estimates lie within a 25% deviation of SB-gf estimates in most catchments. In the wetter catchments where PN used in the two methods differ significantly, GB-GEV estimates are somewhat higher than SB-gf estimates, especially for M100 (see Fig. 10). The largest deviation is seen at Svartevatn, where GB-GEV estimates are 40–60% higher. A natural explanation for this is the elevation gradient for precipitation used in the gridded dataset, which in wet areas such as Svartevatn, is likely to generate serious over-estimation since the elevation gradient is defined as a percentage. The growth factors in SB-gf seem to correspond to a somewhat higher positive  $\xi_a$  compared to the estimated  $\xi_a$  in GB-GEV. Consequently, in the case of GB-GEV > SB-gf for shorter return periods, the longer return periods might correspond quite well. While in the opposite case the difference will grow further with longer return periods.

Figure 11 shows examples of estimates from four catchments: Soneren, Siljan, Aursunda and Roskreppfjord, including empirical values. As these are grid-based empirical values, and

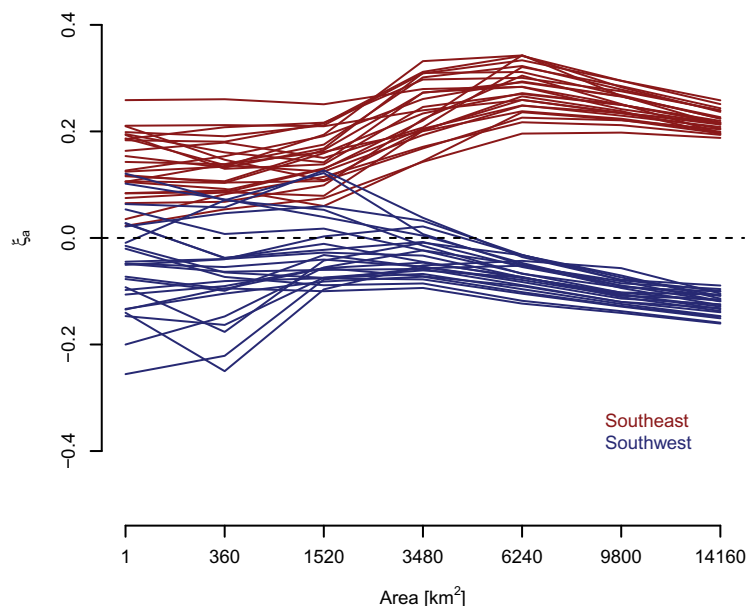
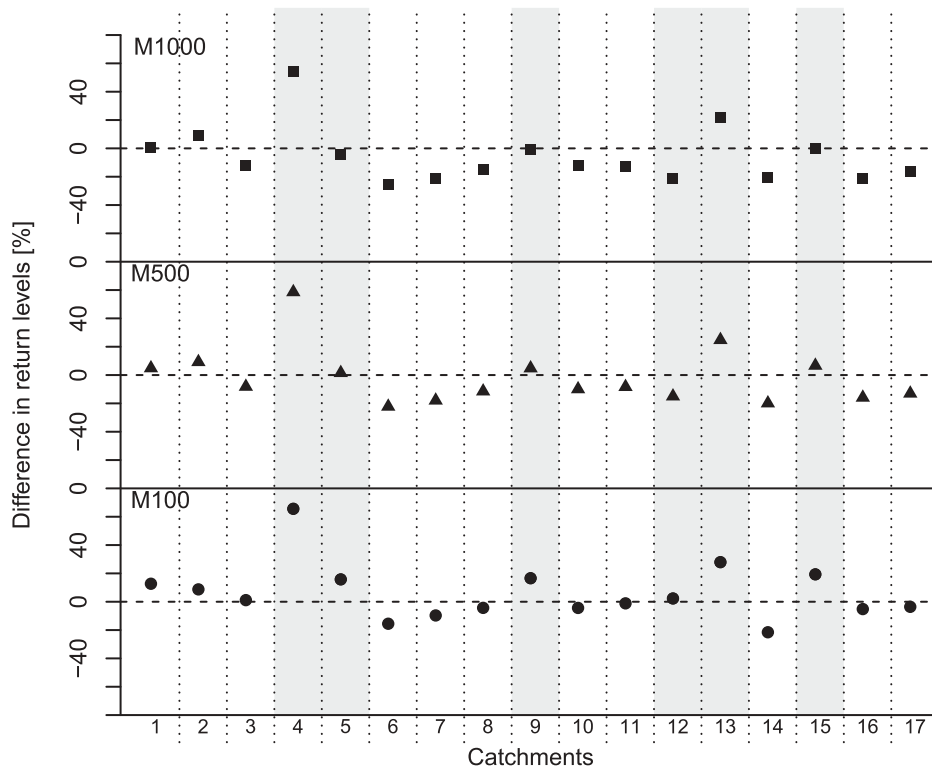
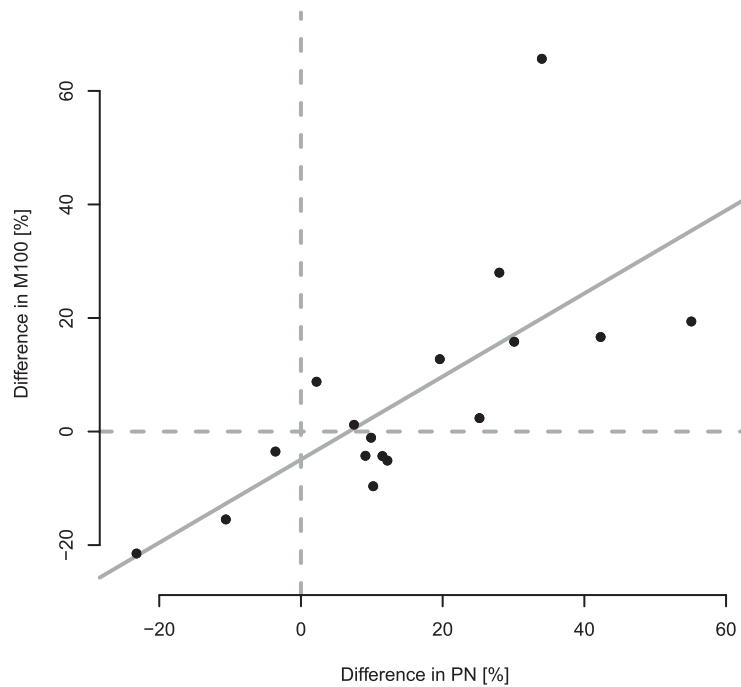


Figure 8.  $\xi_a$  estimated from the gridded dataset, against area size in the Southeast (red) and the Southwest (blue) of Norway.



**Figure 9.** Percentage difference in M100 (circle), M500 (triangle), and M1000 (square) between SB-gf and GBGEV estimates. Grey shading indicates catchments with a large difference in PN used in the two methods.



**Figure 10.** Percentage difference in M100 between SB-gf and GB-GEV estimates, against difference in PN used in the two methods. The grey solid line indicates the result of the linear regression, and the two grey dashed lines indicate no difference between the methods.

thus biased towards GB-GEV, they cannot be applied to determine the better model. The 95% and 99% confidence intervals, indicating the uncertainty in the GB-GEV estimates, are shown in Fig. 11. It must be emphasized that this confidence interval only reflects the uncertainty in the estimation of the GEV

parameters, while additional and unquantifiable uncertainty is associated with the gridded dataset. For longer return periods, SB-gf stays within the confidence intervals of GB-GEV in all catchments, except at Sira where SB-gf moves slightly above the upper confidence level for M1000.

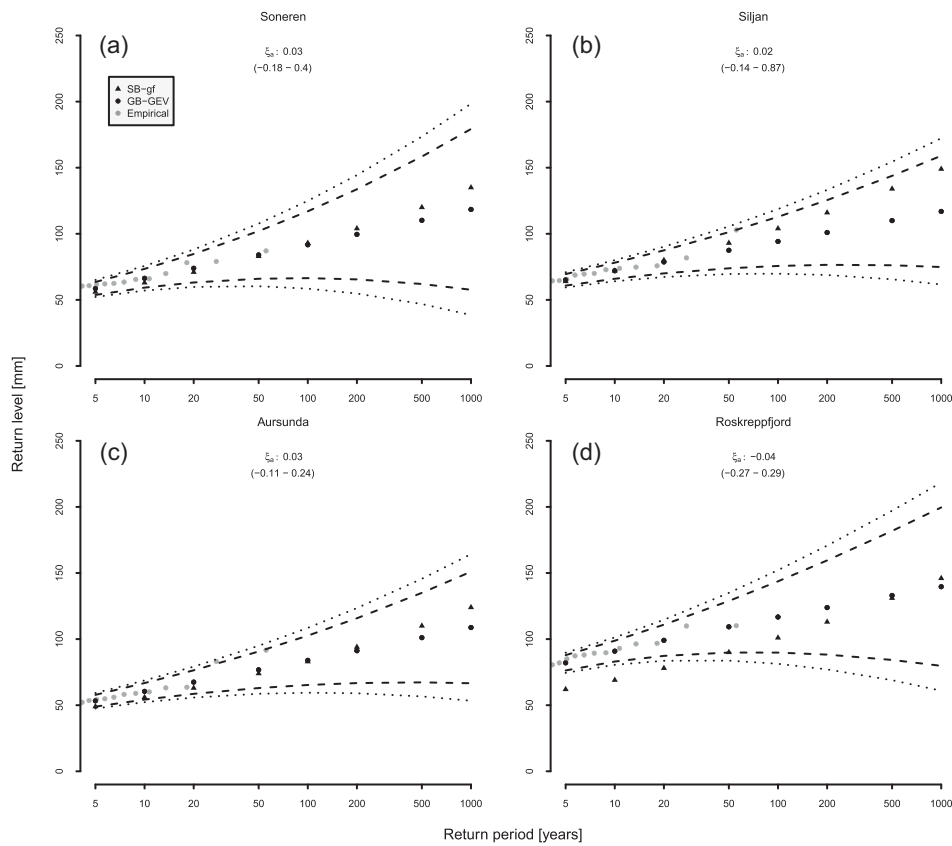


**Figure 11.** Estimated return levels for areal precipitation at: (a) Soneren, (b) Siljan, (c) Aursunda and (d) Roskreppfjord catchments, using SB-gf and GB-GEV. Empirical values are from the gridded dataset. The dashed (dotted) line indicates the 95% (99%) confidence intervals.

Uncertainties in the gridded dataset are likely to influence our estimates, particularly in high elevated and ungauged regions. Another aspect is the vertical precipitation gradient, known to overestimate precipitation at higher elevations. The latter, being defined as a percentage, produces an even greater overestimation of the extreme values. However, extremes in any interpolated dataset are often underestimated due to smoothing, and the relatively sparse station network results in many large precipitation events not being measured because small convective cells may travel between observation sites rather than across them. In catchments located on the borders between different precipitation regimes, the spatial coherence might be reduced both due to the nature of different precipitation systems and the heterogeneous effect of the precipitation gradient. An important part of computing extreme areal precipitation estimates is to be aware of these effects and, while anticipating improved datasets, consider alternative estimation methods in the more uncertain regions.

A more comprehensive study of different precipitation types and their spatial distribution would be an interesting focus for future work. Numerical weather models or statistical pattern recognition (Skaugen 1997) can, for instance, be used to separate frontal from convective precipitation, which could further confirm the effect of precipitation types on the negative shape parameters seen in the Southwest. An analysis of the orographic effect on spatial correlation also remains a subject for future research.

## 4 Conclusions

We propose a new grid-based method, GB-GEV, for estimating extreme areal precipitation in Norway. To the best of our knowledge we are the first to use fine-scale grids for this purpose, and to investigate the behaviour of the GEV  $\xi$  parameter in Norway. Estimates from GB-GEV are compared to estimates from the existing method at MET Norway, SB-gf. Due to large uncertainties and short time series, as well as the absence of areal precipitation measurements, it is difficult to indicate which estimates are better. However, there are relevant and decisive differences between the methods. Our findings can be summarized as follows:

- Grid-based methods are less manual and time-consuming compared to the station-based method, as well as more objective and consistent in terms of input data. In addition, estimates in ungauged catchments are easier to obtain.
- GB-GEV estimates are generally lower than SB-gf estimates, but lie within a 25% deviation in most catchments.
- We have shown that  $\xi_p$  varies spatially in Norway, seemingly depending on dominating precipitations systems and orographic enhancement. For areal extremes the catchment size plays an additional role due to the degree of spatial correlation. We also observe that record length influences the  $\xi_p$  estimates and that the accuracy most likely increases with longer series. Our results suggest that  $\xi_a$

should be modelled according to empirical evidence; however, a more extensive analysis and perhaps additional data sources are required before concluding on a suitable model.

The authors recognize that GB-GEV estimates are dependent on the quality of the gridded dataset. This means that estimates are less robust in areas with few observations and complex topography. Still, GB-GEV estimates will become more accurate as gridded products improve in the future, and the suggested methodology provides more objective and geographically consistent results than the SB-gf method. GB-GEV can also be applied in estimating extreme precipitation from future climate projections.

## Acknowledgements

Valuable feedback from Torill Engen-Skaugen (MET Norway) and the two reviewers is appreciated.

## Disclosure statement

No potential conflict of interest was reported by the authors.

## Funding

We thank the Norwegian Water Resources and Energy Directorate (NVE), Norwegian railway authority (Jernbaneverket) and Norwegian public roads administration (Statens vegvesen) for providing financial support to this study which is part of a PhD project at MET Norway.

## References

- Bell, F.C., 1976. The areal reduction factor in rainfall frequency estimation. Report no. 35 Wallingford, UK: Institute of Hydrology, Report no. 35.
- Blumen, W. ed., 1990. Atmospheric processes over complex Terrain. *Meteorology Monograph no. 45*, American Meteorological Society.
- Caroletti, G.N. and Barstad, I., 2010. An assessment of future extreme precipitation in western Norway using a linear model. *Hydrology and Earth System Sciences*, 14, 2329–2341. doi:10.5194/hess-14-2329-2010.
- Coles, S.G., 2001. *An introduction to statistical modeling of extreme values*. Springer Series in Statistics. London: Springer-Verlag, 45–57.
- Coles, S. and Pericchi, L., 2003. Anticipating catastrophes through extreme value modelling. *Applied Statistics*, 52, 405–416.
- Coles, S., Pericchi, L.R., and Sisson, S., 2003. A fully probabilistic approach to extreme rainfall modeling. *Journal of Hydrology*, 273 (1–4), 35–50. doi:10.1016/S0022-1694(02)00353-0.
- Coles, S.G. and Tawn, J.A., 1996. Modelling extremes of the areal rainfall process. *Journal of the Royal Statistical Society, Series B (Methodological)*, 58 (2), 329–347.
- Cotton, W.R., McAnelly, R.A., and Ashby, T., 2003. Development of new methodologies for determining extreme rainfall. Fort Collins, CO: Colorado State University Final report.
- Engeset, R.V., et al., 2004. Snow map validation for Norway. *Proceedings XXIII Nordic Hydrological Conference 2004*, 8–12 August 2004, Tallinn, Estonia, NHP report, 48 (1), 122–131.
- Førland, E.J. 1986a. Påregnelige ekstreme nedbørhøyder for Jølstra (in Norwegian). *Met.no Report 49/86 KLIMA\**.
- Førland, E.J. 1986b. Påregnelige ekstreme nedbørhøyder for Siljanvassdraget (in Norwegian). *Met.no Report 44/86 KLIMA\**.
- Førland, E.J. 1987. Beregning av ekstrem nedbør (in Norwegian). *Met.no Fagrapport 23/87 KLIMA\**.
- Førland, E.J. 1988. Røssvatn, påregnelige ekstreme nedbørverdier (in Norwegian). *DNMI Report 15/88 KLIMA\**.
- Førland, E.J. 1990. Barduvassdraget, påregnelige ekstreme nedbørverdier (in Norwegian). *DNMI Report 9/90 KLIMA\**.
- Førland, E.J. 1991a. Namsen vassdraget. Påregnelige ekstreme nedbørverdier (in Norwegian). *Met.no Report 40/91 KLIMA\**.
- Førland, E.J. 1991b. Sira-Kvina vassdraget, påregnelige ekstreme nedbørverdier (in Norwegian). *Met.no Report 22/91 KLIMA\**.
- Førland, E.J. 1992. Manual for beregning av påregnelige ekstreme nedbørverdier (Manual for the estimation of PMP, in Norwegian). *Met.no Report 21/92 KLIMA\**.
- Førland, E.J. 1994. Virdnejavri (Altavassdraget), påregnelige ekstreme nedbørverdier (in Norwegian). *Met.no Report 44/94 KLIMA\**.
- Førland, E.J. 1997. Teksalsvassdraget (Fosen), påregnelige ekstreme nedbørverdier (in Norwegian). *Met.no Report 04/1997 KLIMA\**.
- Førland, E.J. and Kristoffersen, D., 1989. Estimation of extreme precipitation in Norway. *Nordic Hydrology*, 20, 257–276.
- Gumbel, E.J. 2004. *Statistics of extremes*. New York: Dover publications. Unabridged republication of the edition published by Columbia University Press, New York, 1958.
- Hanssen-Bauer, I. 1991. Simoavassdraget, påregnelige ekstreme nedbørverdier (in Norwegian). *Met.no Report 43/91 KLIMA\**.
- Hanssen-Bauer, I. 1992. Aursjøen, påregnelige ekstreme nedbørverdier (in Norwegian). *Met.no Report 46/92 KLIMA\**.
- Hanssen-Bauer, I., et al., 2009. Klima i Norge 2100. *Bakgrunnsmateriale til nou klimatilpassing (Climate in Norway 2100, in Norwegian)*, Norsk klimasenter, Oslo.
- Hisdal, H., Roald, L.A., and Beldring, S., 2006. Past and future changes in flood and drought in the Nordic countries. In: S. Demuth et al., eds. *Climate variability and change: Hydrological impacts*. Wallingford, UK: International Association of Hydrological Sciences. IAHS Publ. 308, 502–507.
- Isaksen, K. 2006. Påregnelig ekstremenedbør (felt). Nedbørfelt: Lauvsnesvassdraget, Flatanger (in Norwegian). *Internal met.no report\**.
- Jansson, A., et al., 2007. NORDGRID – a preliminary investigation on the potential for creation of a joint Nordic gridded climate dataset. *Met.no Report 03/2007 Climate*.
- Jenkinson, A.F., 1955. The frequency distribution of the annual maximum (or minimum) values of meteorological elements. *Quarterly Journal of the Royal Meteorological Society*, 81, 158–171. doi:10.1002/qj.49708134804.
- Katz, R.W., Parlange, M.B., and Naveau, P., 2002. Statistics of extremes in hydrology. *Advances in Water Resources*, 25, 1287–1304. doi:10.1016/S0309-1708(02)00056-8.
- Koutsoyiannis, D., 2004a. Statistics of extremes and estimation of extreme rainfall: I. Theoretical investigation. *Hydrological Sciences Journal*, 49 (4), 575–590. Available online at: <http://www.tandfonline.com/doi/abs/10.1623/hysj.49.4.575.54430> doi:10.1623/hysj.49.4.575.54430.
- Koutsoyiannis, D., 2004b. Statistics of extremes and estimation of extreme rainfall: II. Empirical investigation of long rainfall records. *Hydrological Sciences Journal*, 49 (4), 4–610. Available online at: <http://www.tandfonline.com/doi/abs/10.1623/hysj.49.4.591.54424> doi:10.1623/hysj.49.4.591.54424.
- Koutsoyiannis, D. and Baloutsos, G., 2000. Analysis of a long record of annual maximum rainfall in Athens, Greece, and design rainfall inferences. *Natural Hazards*, 22 (1), 29–48. doi:10.1023/A:1008001312219.
- Leadbetter, M.R., Lindgren, G., and Rootzén, H., 1980. *Extremes and related properties of random sequences and processes*. Springer Series in Statistics. New York: Springer-Verlag.
- Mamen, J. 2009. Påregnelig ekstremenedbør (felt). Nedbørfelt: Dam Hoifæt (in Norwegian). *Internal met.no report\**.
- Mamen, J. 2011a. Påregnelig ekstremenedbør (felt). Nedbørfelt: Arendalsvassdraget (in Norwegian). *Internal met.no report\**.
- Mamen, J. 2011b. Påregnelig ekstremenedbør (felt). Nedbørfelt: Røssåga (in Norwegian). *Internal met.no report\**.
- Mohr, M. 2009. Comparison of Version 1.1 and 1.0 of gridded temperature and precipitation data for Norway. *met.no Note 19/2009\**.
- NERC, 1975. *Flood Studies Report, Vol II*. Wallingford, UK: Natural Environment Research Council.
- NVE, 2011. *Retningslinjer for flomberegninger (Guidelines for flood estimations, in Norwegian)*. Retningslinjer nr. 4/2011. Available from:

- [http://www.nve.no/Global/Sikkerhetogtilsyn/Damsikkerhet/Retningslinjer/Retningslinje\\_for\\_flomberegninger\\_2011.pdf](http://www.nve.no/Global/Sikkerhetogtilsyn/Damsikkerhet/Retningslinjer/Retningslinje_for_flomberegninger_2011.pdf)
- Overeem, A., *et al.*, 2010. Extreme value modeling of areal rainfall from weather radar. *Water Resources Research*, 46 (9). doi:10.1029/2009WR008517.
- Papalexiou, S.M. and Koutsoyiannis, D., 2013. Battle of extreme value distributions: a global survey on extreme daily rainfall. *Water Resources Research*, 49 (1), 187–201. doi:10.1029/2012WR012557.
- Pearson, K., 1900. On the criterion that a given system of deviations from the probable in the case of a correlated system of variables is such that it can be reasonably supposed to have arisen from random sampling. *Philosophical Magazine Series 5*, 50 (302), 157–175.
- Prescott, P. and Walden, A.T., 1980. Maximum likelihood estimation of the parameters of the generalized extreme value distribution. *Biometrika*, 67, 723–724. doi:10.1093/biomet/67.3.723.
- Roe, G.H., 2005. Orographic precipitation. *Annual Review of Earth and Planetary Sciences*, 33, 645–671. doi:10.1146/annurev.earth.33.092203.122541.
- Saloranta, T., 2012. Simulating snow maps for Norway: description and statistical evaluation of the seNorge snow model. *The Cryosphere Discussions*, 6, 1337–1366. doi:10.5194/tcd-6-1337-2012.
- Seneviratne, S.I., *et al.*, 2012. Changes in climate extremes and their impact on the natural physical environment. In: *Managing the risks of extreme events and disasters to advance climate change adaptation*. A special report of working groups I and II of the Intergovernmental Panel on Climate Change (IPCC). Cambridge UK: Cambridge University Press, 109–230.
- Skaugen, T., 1997. Classification of rainfall into small- and large-scale events by statistical pattern recognition. *Journal of Hydrology*, 200, 40–57. doi:10.1016/S0022-1694(97)00003-6.
- Skaugen, T., Creutin, J.-D., and Gottschalk, L., 1996. Reconstruction and frequency estimates of extreme daily areal precipitation. *Journal of Geophysical Research*, 101 (D21), 26287–26295. doi:10.1029/96JD01384.
- Svensson, C. and Jones, D.A., 2010. Review of methods for deriving areal reduction factors. *Journal of Flood Risk Management*, 3, 232–245. doi:10.1111/j.1753-318X.2010.01075.x.
- Tveito, O.E., *et al.*, 2005. A GIS-based agro-ecological decision system based on gridded climatology. *Meteorological Applications*, 12 (1), 57–68. doi:10.1017/S1350482705001490.
- Veneziano, D., Langousis, A., and Lepore, C., 2009. New asymptotic and preasymptotic results on rainfall maxima from multifractal theory. *Water Resources Research*, 45 (11). doi:10.1029/2009WR008257.
- Wilks, D.S., 1993. Comparison of three-parameter probability distributions for representing annual extreme and partial duration precipitation series. *Water Resources Research*, 29 (10), 3543–3549. doi:10.1029/93WR01710.
- Wilson, D., Hisdal, H., and Lawrence, D., 2010. Has streamflow changed in the Nordic countries? Recent trends and comparisons to hydrological projections. *Journal of Hydrology*, 394 (3–4), 334–346. doi:10.1016/j.jhydrol.2010.09.010.
- Wilson, P.S. and Toumi, R., 2005. A fundamental probability distribution for heavy rainfall. *Geophysical Research Letters*, 32 (14), doi:10.1029/2005GL022465.
- WMO, 2009. *Manual on Estimation of Probable Maximum Precipitation (PMP)*. WMO-No.1045.
- Yu, C.-K. and Cheng, L.-W., 2008. Radar observations of intense orographic precipitation associated with typhoon Xangsane (2000). *Monthly Weather Review*, 136, 497–521. doi:10.1175/2007MWR2129.1.
- Yu, C.-K. and Cheng, L.-W., 2013. Distribution and mechanisms of orographic precipitation associated with typhoon Morakot (2009). *Journal of the Atmospheric Sciences*, doi:10.1175/JASD-12-0340.1.